Global perspectives on evaluating effective porosity and permeability: Insights from hydrocarbon reservoirs in the Lower Rutba Formation, Sijan Field, Syria

Abdelbaset M. Abudeif [1*✉ ⓘ], Marwa M. Masoud [1✉ ⓘ], Mohammed A. Mohammed [1✉ ⓘ],

Ayoub Y. Alhussain [1✉ ⓘ], Mahmoud A. Abbas [2,3✉ ⓘ]

[1] *Sohag University, Sohag, Egypt*
[2] *University of Naples Federico II, Naples, Italy*
[3] *South Valley University, Qena, Egypt*
Corresponding author: e-mail a.abudeif@science.sohag.edu.eg

Abstract

Purpose. This paper aims to evaluate the petrophysical characteristics of the Lower Rutba Formation in the Sijan Field, Syria, focusing on effective porosity and permeability, and their influence on hydrocarbon productivity. The study intends to develop a practical and cost-effective model for optimizing hydrocarbon recovery, contributing to energy resource sustainability and global energy security.

Methods. The research utilizes log data from 10 wells in the Sijan Field. Sonic, density, and neutron logs were employed to calculate porosity and permeability, while water saturation was estimated using the Archie equation. A comparative analysis across wells was conducted to determine reservoir quality variations and identify high-potential production zones.

Findings. Results revealed significant heterogeneity in petrophysical properties across the field. Wells such as SIJ.110 showed high effective porosity and good permeability, indicating enhanced hydrocarbon storage and flow capacity. In contrast, wells with elevated clay content, such as SIJ.115, displayed low permeability and diminished reservoir quality. Saturation maps effectively highlighted zones with promising production potential.

Originality. The paper introduces a novel integration of log interpretation and mathematical modeling, enabling permeability estimation without core samples. This approach enhances reservoir evaluation, particularly in sandy clay formations, and is adaptable to similar geological settings worldwide.

Practical implications. The study provides a robust and economical framework for assessing reservoir quality. It reduces dependency on core data, supports targeted field development, and promotes sustainable hydrocarbon extraction through improved decision-making in reservoir management.

Keywords: Lower Rutba Formation, effective porosity, permeability evaluation, hydrocarbon reservoirs, sustainable resource management

1. Introduction

Once an oil accumulation is discovered, it is necessary to characterize the reservoir as accurately as possible to calculate reserves and determine the most effective way to recover as much oil as economically feasible. Reservoir characterization integrates many geological and geophysical data, most notably well logs. One of the basic requirements for the commercial accumulation of hydrocarbons is the existence of a reservoir. In theory, any rock can serve as a reservoir for oil or gas. In practice, sandstones and carbonates contain the central known reserves, although fields are found in shales and diverse igneous and metamorphic rocks [1].

Undoubtedly, the massive technical development and information age we are witnessing today have borne fruit in the field of well measurements, which has increased its superiority and success. This development is represented by the innovation of well measuring devices that can be used even in wells with small diameters, as well as the develop-

ment of methods for processing well data by using the latest computers to accomplish this work and within a short period through programs that are also at a high level of efficiency in dealing with a considerable amount of well data, and the development of communications technologies ensures the transfer of all data from the measurement site to any processing center in the world [2].

Well logging, or formation evaluation, is crucial to oil and gas exploration and drilling. This process provides critical insights into geological formation characteristics, including porosity, permeability, fluid saturation, rock types, and the thickness of productive zones.

Accurately characterizing the reservoir after identifying an oil accumulation is essential for estimating reserves and devising efficient extraction strategies to maximize economic recovery. Reservoir characterization integrates extensive geological and geophysical data, with well logs being a primary source of information [3].

This study focuses on a medium-sized field in the Euphrates Basin, situated within Syrian territory. Syria occupies a small portion of the northwestern edge of the Arabian Plate [4]. The Euphrates Basin is one of Syria's most productive oil regions, with a daily crude oil output of approximately 400000 barrels, ranging from light to heavy oil. In particular, this research examines the petrophysical properties of the Rutba Formation in the Sijan Field, located in Deir Ez-Zor, Syria, as a critical step toward understanding and evaluating oil reservoirs in this area [5].

Due to its significant hydrocarbon potential, the Euphrates Graben in Syria has been a focal point for numerous geological, structural, and geophysical studies. Below are the most important studies and research on the Euphrates Graben.

Studies conducted by Cornell University on the geological and tectonic development of Syria. This study included extensive research to determine the development of the entire geological structure constituting the Syrian lands. Where it has studied the development of the Euphrates Graben, the shapes of the faults affecting it, their directions, the geological times, the tectonic movements that led to the formation of the structure of the graben, the accumulated sedimentary thicknesses in it, and the changes that occurred to it as a result of the fault and erosional processes [6].

3D seismic studies that the Syrian Oil Company carried out. The seismic studies carried out in the region led to determination of the deep geological structure, the faults spread in the region, the faults that led to the closure of the fields structure and the formation of the traps, and the throw of the main fault that prevented the migration of oil in the shallower direction, as well as determining the general shape of Rutbah Formation [7].

A sedimentological and petrophysical study of the Rutbah Formation in Euphrates Graben. This study dealt with microscopic and laboratory research on the Rutbah Formation in the Euphrates Graben. It also determined its petrophysical properties and a granular description of the studied slices from several wells spread throughout the Rutbah Formation. The sedimentary environments that led to their formation helped give a general and good idea about the lithological nature and storage properties of the Rutbah Formation [8].

The behavior of fluids within rock voids is pivotal in addressing many challenges related to oil field development and production [9]. Two key properties, porosity and permeability, are central to this understanding. Porosity measures the void space within rocks, while permeability assesses the rock's ability to transmit fluids. These properties are fundamental to determining the types and quantities of fluids, fluid flow rates, and recovery estimates. Porosity and permeability measurement techniques form a substantial part of the technical literature in the oil industry.

Engineers primarily focus on rock porosity when estimating oil and gas quantities in a reservoir. Conversely, permeability is critical for addressing production rate challenges [10]. While permeability and porosity are generally correlated, particularly in sand formations, this relationship may not hold for all rock types [11].

The Rutba Formation in the Euphrates Basin is a significant geological unit due to its extensive width and thick sand deposits, which possess favorable storage properties. As a result, it has been a focal point of numerous studies [1]. This research emphasizes the role of effective porosity and permeability in assessing reservoir quality and production potential. By analyzing data to identify zones with optimal storage and fluid transmission capacity, this study supports the development of strategies for sustainable energy resource management. Additionally, it aims to provide a practical model applicable to similar fields, enhancing the efficiency of oil resource exploitation and contributing to the national economy.

2. Geologic setting of Syria, including the study area

Syria is situated in the northwestern part of the Middle East, spanning latitudes 32°19′ to 37°25′ N and longitudes 35°43′ to 42°25′ E (Fig. 1a). It is bordered to the north by Turkey, to the east by Iraq, to the south by Jordan and Palestine, and the west by Lebanon and the Mediterranean Sea [12].

The tectonic structure of Syria is an extension of the Arabian Peninsula's tectonic framework and features a combination of uplifts, depressions, and mountain ranges (Fig. 1b). The uplifts include the Rutbah Uplift, Rawdah Uplift, Najd Aleppo Uplift, Qamishli Uplift, and Sinjar Uplift. The region also contains five notable depressions: the Jabal al-Arab Depression, Dou Depression, Euphrates Graben, Homs Depression, and Abdul Aziz Depression [13]. Additionally, Syria is characterized by two prominent mountain ranges: the Palmyra Range and the Coastal Mountain Range [14].

Diverse sedimentary and volcanic rocks characterize the geology of Syria. Sedimentary rocks, primarily carbonates with lesser amounts of marly, clastic, and evaporite deposits, dominate the landscape, spanning ages from the Upper Triassic to the Neogene (Fig. 1c). These sedimentary formations cover approximately 75% of the country's surface area. The remaining geological features include volcanic rocks, such as basalt flows within Upper Jurassic and Lower Cretaceous formations, and extensive basalt shields covering large areas in southwestern, central-western, and northeastern Syria. These basaltic rocks date back to the Neogene-Quaternary period. Additionally, ophiolitic rock masses and associated volcanic rocks are found in northern and northwestern Syria, further enriching the country's geological complexity [15].

2.1. Euphrates Graben location

The eastern part of the Euphrates Graben is located in Iraqi territory. In contrast, its western part is located in Syrian territory (Fig. 1d). It extends about 160 km from western Iraq to central Syria [14]. This depression is bordered to the south by the Rutbah Uplift, to the west by the Aleppo Uplift and the Palmyra Mountains. To the north, the Sinjar, Abdul Aziz and Twal Al-Aba peaks are distributed [15].

2.2. Overview of the Euphrates Graben system

It is located above the structures of the slope of the Arabian plate, with both its fixed and mobile parts [16]. This depression arose due to the divergent tectonic activity in the period extending from the Middle Cretaceous to the Late Cretaceous, where tectonic activity stopped with the beginning of the convergence between the Arabian and Anatolian plates.

This depression is filled with large thicknesses of marine and continental Neogene sediments, and deep drilling results indicate that Cretaceous sediments are placed above Carboniferous sediments (Fig. 2). The Euphrates fault system is formed from a complex network of normal and branching faults. Late Cretaceous fault structures in southeastern Syria were buried under Cenozoic sediments to about 5 km and contributed to large regional oil reserves [15].
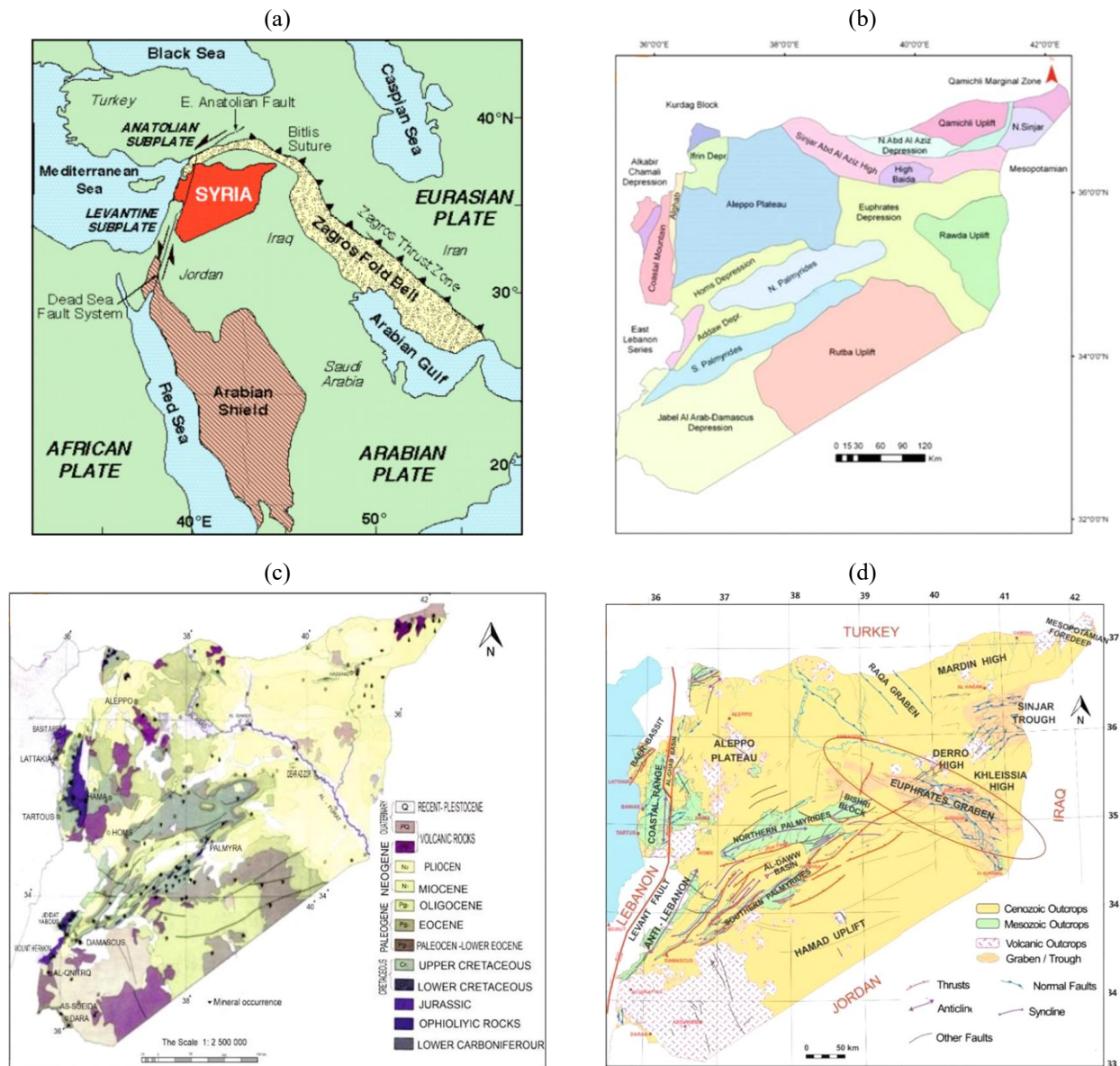
(a)

(b)

(c)

(d)

Figure 1. Tectonic and geological framework of Syria: (a) Syria's location within the regional tectonic setting [17]; (b) structural map showing key units such as the Aleppo Plateau and Euphrates Depression [17]; (c) geological map illustrating rock units by age and type [18]; (d) tectonic-geological map highlighting faults and prominent features like the Euphrates Graben and Palmyra Fold Belt [15]
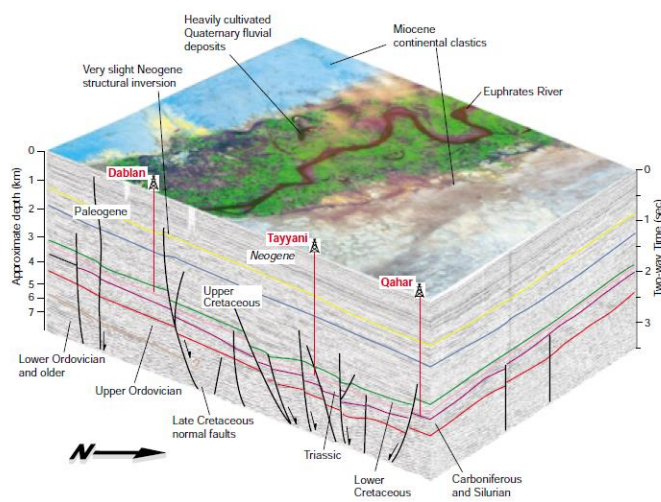

Figure 2. A three-dimensional visualization integrating geological and seismic data to provide insight into the structure and stratigraphy of the Euphrates Graben [6]

2.3. Stratigraphic column of the Euphrates Graben

Figure 3 represents the stratigraphic column of the eastern region of Syria, including the Rutbah Formation. Below is a detailed description of key formations within the studied area.

Al-Judea Formation. This formation dates back to the Lower Cretaceous and is subdivided into two distinct parts within the Euphrates Graben. Upper Al-Judea Formation has a sandy rock consisting of sandstone and clay, and Lower Carbonate Al-Judea Formation is composed of crystalline carbonates like limestone and dolomite [19].

Rutbah Formation. The Rutbah Formation is one of Euphrates Graben's most significant geological units due to its broad distribution and substantial sand deposits with excellent storage properties. Consequently, it has been the focus of numerous studies. This formation comprises quartzite, clay, and clayey sandstone successions and is divided into two central units, Upper Rutbah and Lower Rutbah formations.
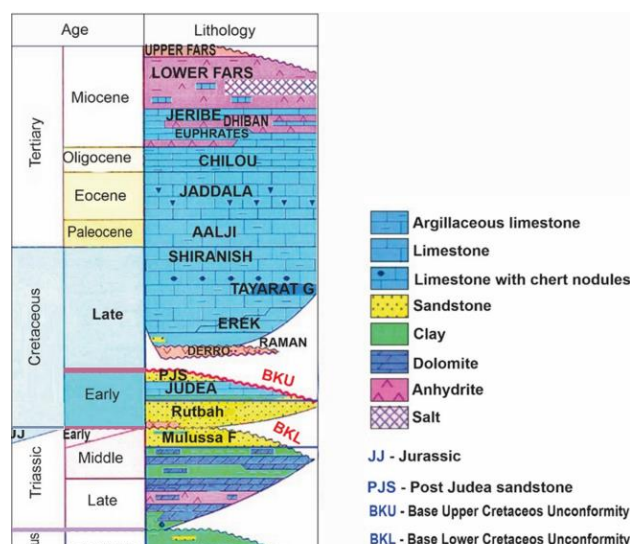
Figure 3. The stratigraphic column spans geological time from the Cambrian-Ordovician to the Tertiary period, presenting the lithological distribution and stratigraphic relationships of formations in the Euphrates Graben. The diagram includes key markers such as unconformities and lithological variations, with color coding and patterns to differentiate rock types [20]

Sediments from the Upper Rutbah Formation are attributed to the Lower Cretaceous age. They predominantly consist of shale with minor sandstone content; the rocks are generally muddy and, in some cases, slightly calcareous. Lower Rutbah Formation. Also dated to the Lower Cretaceous, this unit mainly comprises sandstone interspersed with minor shale deposits [1].

Mulussa Formation. This formation belongs to the Upper Triassic age and comprises sandstones and clay deposits [20].

2.4. Geology and structures of Sijan Field

Sijan Field is located in the north-eastern part of the Euphrates Graben in eastern Syria (Fig. 4). The field is approximately 20 km long by 5 km wide and is a complex of 11 faulted dip closures with different fluid levels (ranging from 2716 to 3090 m). Integration of the structural model of the Sijan Field into the understanding of the regional structural concepts has been attempted. A very comprehensive analysis of the structural history and characteristics of the Middle Euphrates Graben can be found in "Structural analysis and kinematic framework of the Euphrates Graben, Eastern Syria" by Koopman [7]. Figure 5 reveals a highly complex fault system with four dominant trends: Palmyrid, Khabour, Mesopotamian, and Euphrates. These fault systems are interlocking, indicating simultaneous tectonic activity that shaped the subsidence and faulting in the region. The structure of the faults and the interaction between the different trends have significant implications for geological processes, including hydrocarbon exploration, as the faults may control the formation of traps and migration pathways.

A concise interpretation of Figures 4 & 5 highlights that the Sijan Field occupies a structurally significant position within the northeastern sector of the Euphrates Graben.
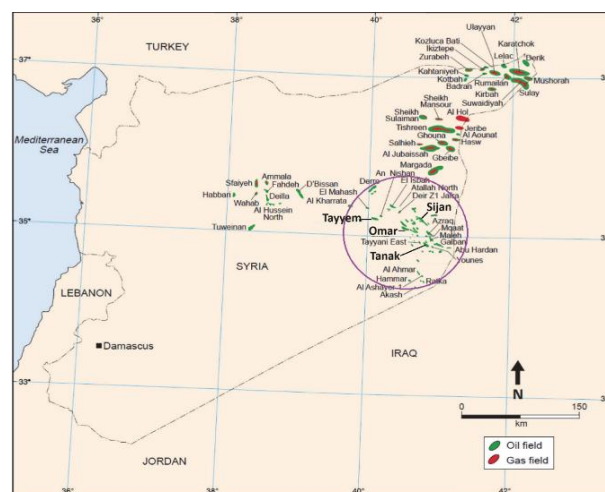

Figure 4. Euphrates Graben fields with an explanation of the location of the Sijan field [21]
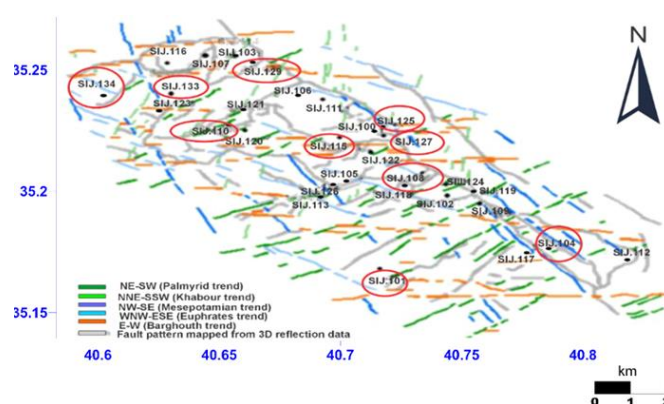

Figure 5. Structural situation in the Euphrates Graben [7]

Figure 4 shows its spatial distribution relative to nearby oil and gas fields, indicating its strategic location within a tectonically active corridor. Figure 5 further illustrates the field's structural complexity, with multiple intersecting fault trends, namely Palmyrid, Khabour, Mesopotamian, and Euphrates, converging in the area. These intersecting trends create faulted dip closures and compartmentalization within the Sijan Field, directly influencing fluid distribution, trap formation, and hydrocarbon migration. This structural interplay is a key control on the reservoir architecture and productivity of the field.

3. Methodology

Data was obtained for 10 wells penetrating the Rutbah Formation in the Field of study, where the wells will be studied and the petrophysical properties of each well will be determined, and this depends mainly on the experience of the interpreter in understanding the executed well probes and their responses according to the following steps:

– uploaded the digitally recorded well data in LAS format to the software for processing and interpretation to facilitate the evaluation of petrophysical properties. Choosing the appropriate logs, single or multiple, according to the objective to be calculated;

– using appropriate logs to determine the upper and lower limits of the Rutbah Formation;

– gamma-ray measurements are used to identify the different types of lithology.

Calculate the volume of the shale and then exclude the non-productive zones. The presence of shale within reservoir rocks has a significant impact on the hydrocarbon extraction process. Determining the shale volume is essential for distinguishing between highly productive sandstone zones and mixed zones with elevated shale content. This calculation is also crucial for accurately evaluating effective porosity and permeability, enabling more precise planning and execution of hydrocarbon extraction operations [22]. Shale volume is derived from measured gamma-ray values using Equation (1):

$$V_{sh} = I_{GR} = \frac{GR_{\log} - GR_{\min}}{GR_{\max} - GR_{\min}},$$ (1)

where:

V_{sh} – volume of shale;
I_{GR} – gamma ray index;
$GR_{\log}$ – gamma ray reading of formation;
$GR_{\min}$ – minimum gamma ray;
$GR_{\max}$ – maximum gamma ray;

Calculating the total and effective porosity through porosity measurements (density and neutron logs).

3.1. Density porosity

Density porosity is derived from formation density logs, which indicate the rock's capacity to retain fluids such as water, oil, or gas. This property is typically expressed as a relative value or percentage and can be calculated using Equation (2) [11]:

$$\phi_D = \frac{\rho_{ma} - \rho_b}{\rho_{ma} - \rho_{fl}},$$ (2)

where:

ϕ_D – density derived porosity;
ρ_{ma} – matrix density;
ρ_b – formation bulk density;
ρ_{fl} – fluid density.

The values of ρ_{ma} and ρ_{fl} are considered fixed, based on the type of rock, as specified in the density table provided by Schlumberger (Table 1).

Table 1. Typical values for the density of rocks and fluids [11]

Lithology / Fluid	Formula	ρ_{ma} / ρ_{fl} (g/cm^3)
Sandstone	SiO_2	2.644
Limestone	$CaCo_3$	2.710
Dolomite	$CaCo_3MgCo_3$	2.877
Anhydrite	$CaSo_4$	2.960
Oil	–	0.850
Fresh Water	–	1

Density porosity in clay rocks is usually low because the clay contains small, interlocking pores and the presence of water associated with clay minerals. Sandstone has a higher density porosity than clay rocks, especially if it is clean and free of clay; this reflects the ability of sandstone to hold fluids such as oil and gas [23].

3.2. Neutron porosity

Neutron porosity is measured by detecting the number of thermal neutrons or gamma rays emitted from the formation. The reflected neutron count is directly proportional to the hydrogen content within the rock. These measurements are then interpreted to estimate porosity. Since hydrogen is commonly found in water or hydrocarbons within geological formations, an increase in thermal neutron count corresponds to higher porosity.

Sandstones, being medium-grained rocks, typically contain pores filled with water or hydrocarbons, resulting in neutron porosity readings that closely match their actual porosity. In contrast, shales are rich in clay minerals and exhibit high neutron porosity due to the significant hydrogen content chemically bound to water within the clay minerals. This characteristic often leads to higher neutron porosity readings in shales than pure sandstones [24].

3.3. Total porosity

Neutron-Density Porosity (N-D Porosity): it combines neutron porosity and density measurements to evaluate total and net porosity in rocks accurately. This method enhances the precision of porosity assessments and can be calculated using Equation (3) [25]:

$$\Phi_{N-D} = \frac{\phi_N + \phi_D}{2},$$ (3)

where:

ϕ_N – neutron porosity;
ϕ_D – density porosity.

3.4. Total porosity

Calculating the effective porosity provides an accurate estimation of the ability of rocks to transport fluid, which is a critical step in assessing the quality of shale reservoirs [26]. Using total porosity, shale volume, and shale porosity, the effective porosity can be accurately calculated using Equation (4):

$$\Phi_e = \Phi_{total} - \Phi_{sh} \cdot V_{sh},$$ (4)

where:

Φ_e – effective porosity;
Φ_{total} – total porosity;
Φ_{sh} – porosity resulting from the presence of shale.

Determining the permeability through the core information to infer the relationship between the permeability and porosity, and applying it to all wells to calculate the unknown permeability:

$$\log K = b \cdot \phi - c,$$ (5)

where:

b and c – constants.

Determining the value of the resistivity of formation water R_w using the picket plot that links the values of the effective porosity and the measured depth resistivity.

Conducting a correlation between the studied wells within the Rutbah Formation. Calculating the parameters needed to solve Archie's equation. Calculating water saturation, an essential measure for estimating the amount of hydrocarbon that can be extracted from the reservoir, is done using Archie's relationship, Equation (6) [27]:

$$S_w^n = \frac{a}{\phi^m} \cdot \frac{R_w}{R_t},$$ (6)

where:

S_w – water saturation;
R_w – water resistivity;
R_t – true resistivity;
ϕ – porosity of formation;
m – cementation exponent (for sandstone $m = 1.72$ according to Al-Furat Petroleum Company);
a – tortuosity factor (commonly set to 1.0);
n – saturation exponent (for sandstone, $n = 1.86$ according to Al-Furat Petroleum Company).

Calculating hydrocarbon saturation.

After calculating the water saturation, the hydrocarbon saturation is deduced through Equation (7) [27]:

$$S_h = 1 - S_w. \tag{7}$$

Evaluating the hydrocarbon potential of the Sijan field.

4. Results and discussion

4.1. Calculating shale volume

Gamma-ray values in the Lower Rutba Formation generally exhibit a decreasing trend, with only a few localized anomalies. Shale volume was calculated for the entire formation, and intervals with elevated shale content were excluded from further reservoir analysis. To apply Equation (1), the maximum and minimum gamma-ray values were identified and used in conjunction with the measured gamma-ray readings at each depth point. Equation (1) was applied consistently across all wells in the Lower Rutba Formation to determine shale volume (Figs. 6a-e).

Figure 6 visually compares shale volume distribution in five representative wells (SIJ.115, SIJ.101, SIJ.110, SIJ.133, and SIJ.134). The logs reveal significant variability in shale content among the wells. For example, well, SIJ.115 (Fig. 6a) shows a consistently high shale volume, particularly in the upper sections, indicative of reduced reservoir quality and lower permeability. In contrast, wells SIJ.110 and SIJ.133 (Figs. 6c & 6d) are characterized by dominant sand intervals with lower shale content, reflecting more favorable reservoir conditions. This visual assessment reinforces the quantitative shale volume analysis and supports the identification of cleaner, sand-dominated zones with higher hydrocarbon potential. The average shale volume calculated for each well is presented in Table 2.

Table 2. Average values of shale volume for each well

Well name	SIJ.101	SIJ.110	SIJ.115	SIJ.133	SIJ.134
V_{sh}, %	20	20	24	22	19

4.2. Calculating porosity

Calculating the total porosity in lower Rutbah requires using a set of well logs to analyze the data accurately. Using density logging and neutron logging can provide an accurate estimation of the total and effective porosity, which leads to evaluating the ability of rocks to store and transport fluids.
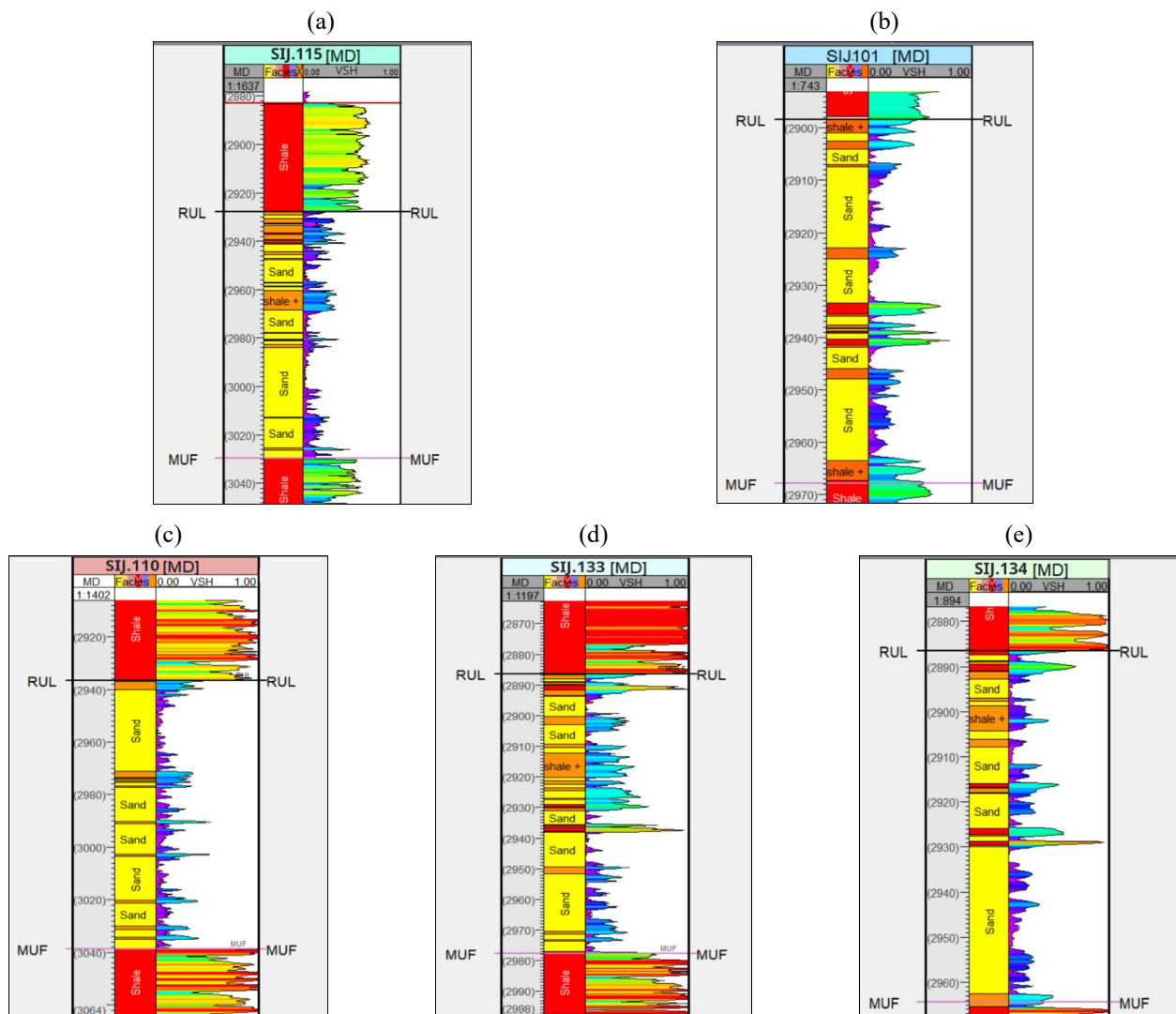

Figure 6. Shale volume distribution in the Lower Rutba Formation for five representative wells: (a) SIJ.115; (b) SIJ.101; (c) SIJ.110; (d) SIJ.133; (e) SIJ.134. The logs illustrate variability in shale content across the formation, highlighting zones of high and low clay concentration, which reflect differences in reservoir quality and sand dominance

Figures 7a-e show the calculation of both the density porosity (PhiDen) and the neutron porosity (PhiNeu) in addition to the calculated total porosity (PhiT) and effective porosity (PhiE).

The porosity values are generally not the same, but are characterized by their change within the reservoir rock. Consequently, an average value represents the total porosity in the formation. Neutron porosity can be determined directly from the neutron logs, while density porosity is calculated using Equation (2) in the lower Rutbah sand zone.

Calculating the effective porosity provides an accurate estimation of the ability of rocks to transport fluid, which is a critical step in assessing the quality of shale reservoirs [26]. Using the total porosity calculated from Equation (3), shale volume, and shale porosity, the effective porosity can be accurately calculated using Equation (5).
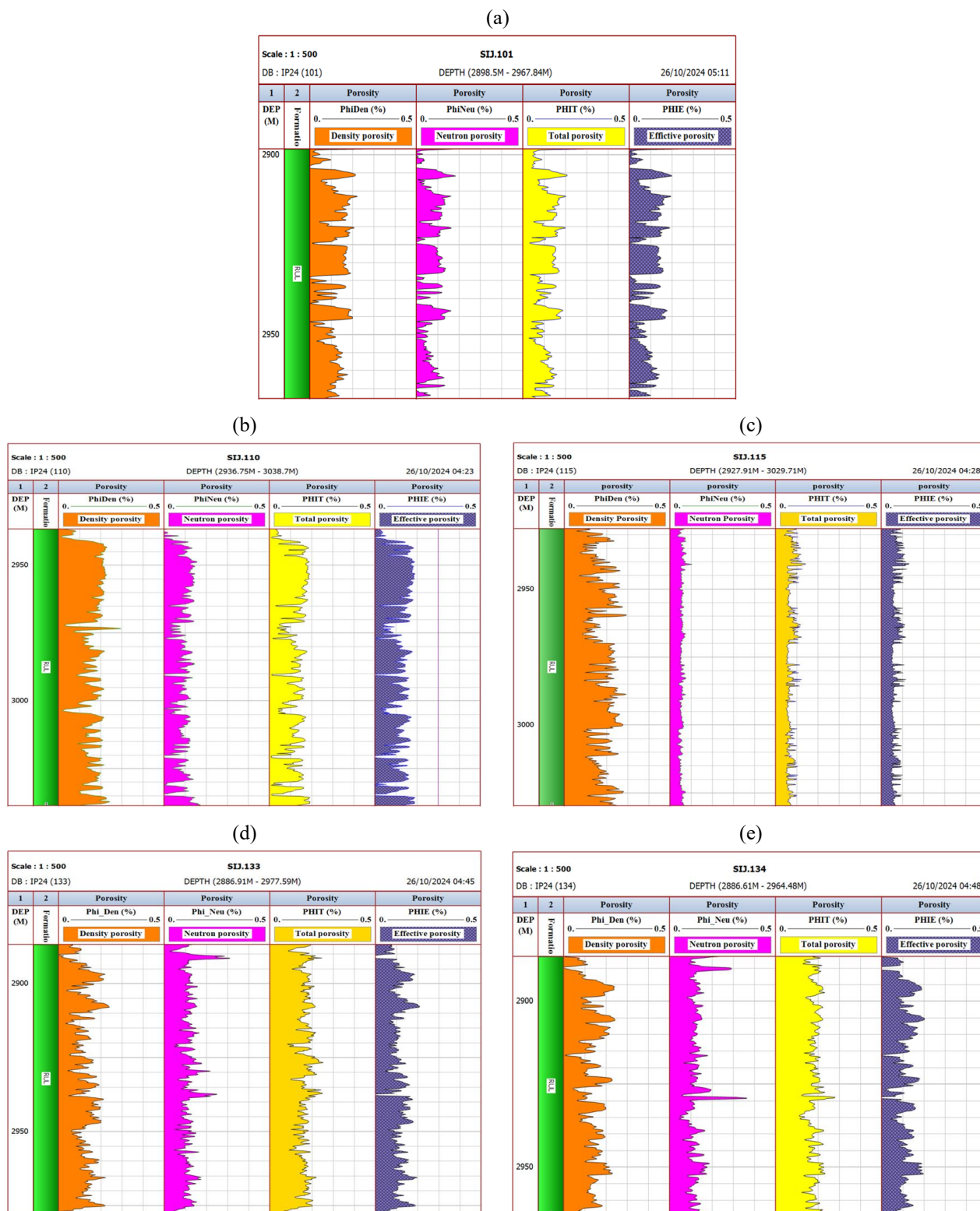

Figure 7. Porosity log responses in the lower Rutbah Formation from selected wells: (a) SIJ.101 well; (b) SIJ.110 well; (c) SIJ.115 well; (d) SIJ.133 well; (e) SIJ.134 well. The logs illustrate various porosity types, including density porosity, neutron porosity, total porosity (PHIT), and effective porosity (PHIE)

Calculating all types of porosities (density, neutron, total, and effective) for all wells is shown in the Figs. 7a-e. The average values of different porosities for each well are in Table 3.

Table 3. Average values of different porosities for each well

Well	SIJ.101	SIJ.110	SIJ.115	SIJ.133	SIJ.134
ϕ_D	12.0	16.8	18.6	12.7	14.0
ϕ_N	12.2	9.4	5.5	11.7	12.5
ϕ_t	12.1	13.1	12.0	12.2	13.2
ϕ_e	10.5	12.6	8.5	11.0	11.3

4.3. Calculating permeability

For a rock to be permeable, it must contain connected pores, and there is an approximate indirect relationship between permeability and porosity. In general, high permeability of rocks means that porosity is high.

Using the information obtained from the core samples of SIJ.115 well [28], which includes porosity and permeability values measured directly from the rock core, an empirical equation was created between the permeability and the porosity. The points cluster in the upper left half of the graph (Fig. 8), indicating that as porosity increases, permeability increases, and as porosity decreases to less than 10% permeability begins to decline significantly. Equation (5) appears on the graph (Fig. 8) and expresses the relationship between porosity ϕ and permeability K. The correlation coefficient R indicates the degree of strength of the relationship between porosity and permeability. A value of 0.6384 indicates a moderate to strong relationship between the two variables, k and ϕ.
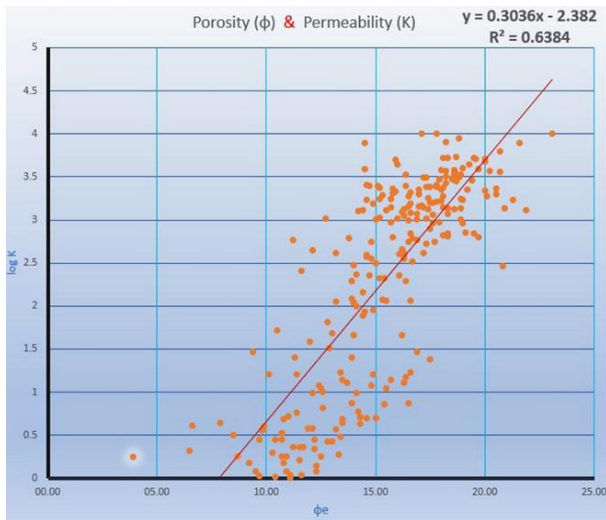

Figure 8. The relationship between porosity and permeability in the Lower Rutba Formation was derived using core analysis data from the SIJ.115 well. The analysis resulted in the empirical equation: log K = 0.3036 ϕ – 2.382", where b = 0.3036 and c = 2.382

The derived empirical equation (Fig. 8) was employed to calculate the permeability in all wells except for SIJ.115, where permeability was determined directly from core sample measurements. This equation incorporates permeability as the unknown variable, while the previously calculated porosity for the Lower Rutba Formation in the target wells serves as an input. The other parameters ($b = 0.3036$ and $c = 2.382$) were obtained from Figure 8.

Consequently, Equation (5) is transformed into (8):

$$\log K = 0.3036 \cdot \phi - 2.382 \,. \qquad (8)$$

The permeability was calculated in all wells, and the average values are shown in Table 4. Figures 9a-e present the effective porosity (PHIE) and permeability (PERM) logs for five wells (SIJ.101, SIJ.110, SIJ.115, SIJ.133, and SIJ.134) within the Lower Rutbah Formation. The figure demonstrates an apparent vertical and lateral variability in both properties across the wells.

Table 4. Average permeability values for each well

Well	SIJ.101	SIJ.110	SIJ.115	SIJ.133	SIJ.134
K, mD	921	1032	626	449	882

Notably, wells SIJ.110 and SIJ.115 exhibit relatively higher permeability values, reaching up to several hundred millidarcies (mD), coinciding with elevated effective porosity zones. These intervals are potential reservoir zones, reflecting good pore connectivity and fluid flow capacity. In contrast, wells SIJ.133 and SIJ.134 show lower and more scattered permeability values, despite moderate effective porosity in some intervals, possibly indicating poor pore throat connectivity or secondary cementation effects.

Overall, the correlation between higher effective porosity and increased permeability in certain zones supports the interpretation that the Lower Rutbah Formation contains heterogeneous reservoir quality, with select intervals exhibiting promising petrophysical characteristics. These findings align with the overall objective of evaluating reservoir potential and help delineate the most prospective zones for further investigation and potential development.

4.4. Porosity and permeability correlation of the Lower Rutbah

4.4.1. Lower Rutbah correlation for porosity

Looking at the data showing the distribution of porosity (PHIE) across the studied wells (SIJ.101, SIJ.110, SIJ.115, SIJ.133, SIJ.134), it is clear that there is a variation in the ability of the rocks to store fluids. Well SIJ.110 shows the highest porosity levels, reflecting an ideal rock formation for hydrocarbon storage, followed by wells SIJ.133 and SIJ.134, which have relatively high porosity, making them a promising area for production. In contrast, well SIJ.101 records medium porosity, which may limit its storage efficiency, while well SIJ.115 shows the lowest porosity levels among the studied wells, making it the least efficient in terms of storage capacity (Fig. 10).

Figure 11 represents the distribution of effective porosity in the reservoir, with dark colors (dark purple) in the northwestern part of the area indicating high porosity values of up to 12%, as shown in the area of well SIJ.110. In contrast, light colors (pink) reflect lower values, such as 8.5% near well SIJ.115. The figure also indicates that the areas around well SIJ.101 show moderate porosity, indicating different rock properties or a heterogeneous rock distribution. Geologically, areas of high porosity indicate rocks with significant hydrocarbon storage and transport capacity and may be associated with favorable depositional environments or geological processes that have improved pore connectivity.

In contrast, areas of low porosity are associated with higher shale content or have been subjected to compaction processes that have reduced porosity.
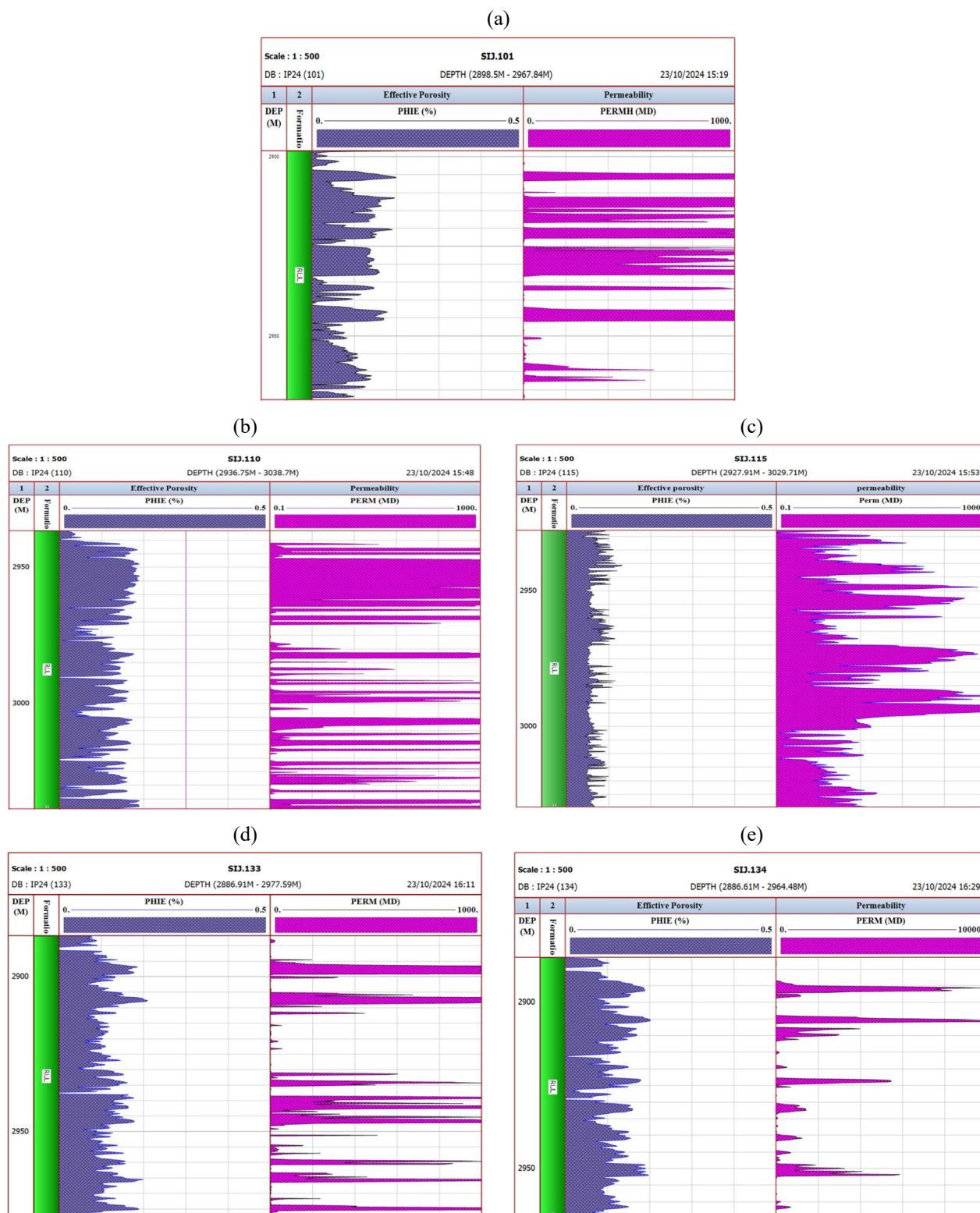
Figure 9. Effective porosity (PHIE) and permeability (PERM) logs for the Lower Rutbah Formation in selected wells: (a) SIJ.101; (b) SIJ.110; (c) SIJ.115; (d) SIJ.133; (e) SIJ.134. The logs highlight the vertical variations and heterogeneity in reservoir quality, where intervals with higher effective porosity generally correspond to zones of enhanced permeability, indicating potential reservoir targets

In addition, the closeness of the contour lines indicates a rapid change in porosity values within a small area, reflecting a significant variation in rock properties, and may be associated with changes in rock quality or formations. The spacing of the contour lines indicates a gradual and slow change in porosity values, indicating a relative homogeneity of the rocks in that area.

In practice, the SIJ.110, SIJ.133 and SIJ.134 well areas were observed to be the most porous, indicating high fluid storage potential. In contrast, the areas surrounding the SIJ.115 and SIJ.101 wells have lower porosity and may require more advanced technology to increase productivity.
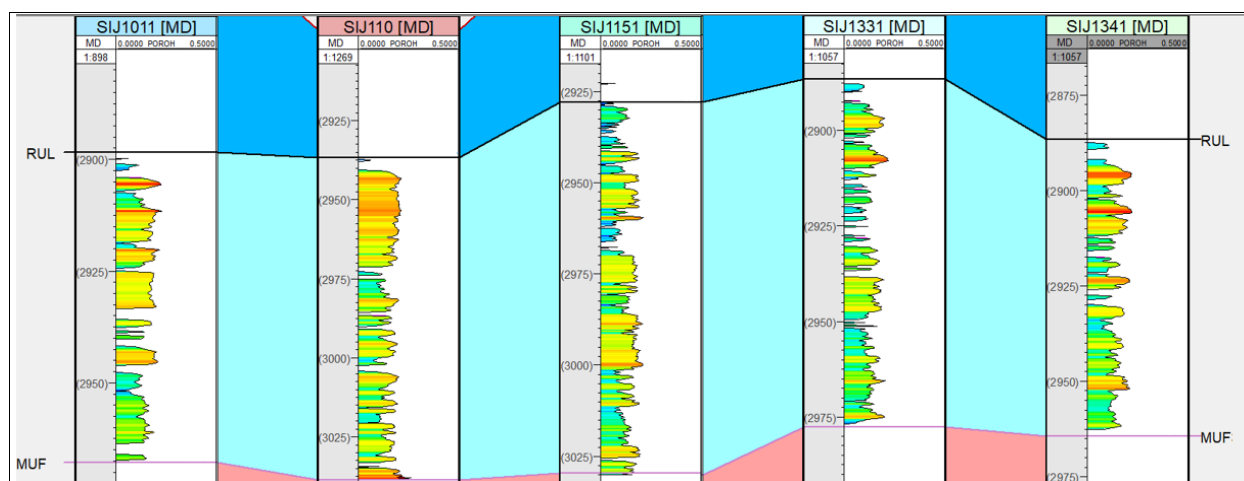
Figure 10. Correlation of porosity in lower Rutbah Formation, wells (SIJ.101-SIJ.110-SIJ.115-SIJ.133-SIJ.134)
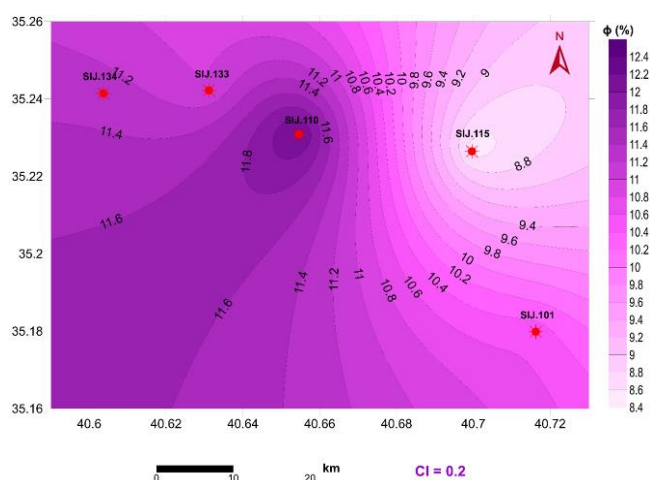

Figure 11. Contour map of the distribution of porosity in the lower Rutbah Formation, Sijan Field

4.4.2. Lower Rutbah correlation for permeability

Vertical comparison of permeability across the studied wells reflects variation in the ability of the rocks to allow fluid passage (Fig. 12). Wells SIJ.110 and SIJ.101 show the highest permeability values compared to the rest of the wells, indicating the presence of wide and connected rock channels that allow fluids to flow easily, making them the most promising locations in terms of production. Well SIJ.134 records medium to high permeability in some layers, making it suitable for production but with less efficiency. In contrast, well SIJ.115 and well SIJ.133 show relatively low permeability, which may limit their production efficiency and indicate less permeable rock formations.

There is a variation in permeability between wells (Fig. 13), with the highest permeability recorded in wells SIJ.110, SIJ.134 and SIJ.101, making these wells the most efficient for production, as shown by the dark green color gradient in the contour map.
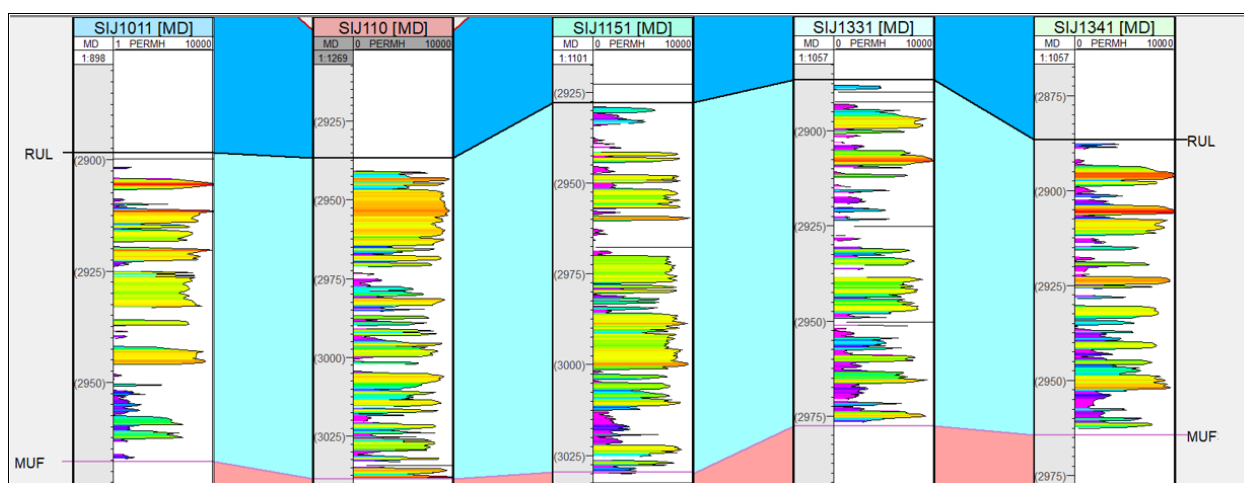

Figure 12. Correlation of permeability in lower Rutbah Formation, wells (SIJ.101-SIJ.110-SIJ.115-SIJ.133-SIJ.134)

On the other hand, permeability decreases significantly in wells SIJ.115 and SIJ.133, and these wells are shown in the light green areas, reflecting less efficient reservoir properties.

The closeness of the contour lines in some areas indicates a considerable variation in rock properties, while their spacing reflects a relative homogeneity in permeability. This spatial gradient suggests that the northwest represents the most productive area of the field, while the southeast is less so. Geologically, high permeability areas may be due to well-connected sand layers or primary flow channels. In contrast, areas of low permeability may represent clay layers or tectonic effects that have affected the distribution of porosity.

4.5. Water and hydrocarbon saturation evaluation

4.5.1. Calculating the water saturation

Calculating water saturation (S_w) is a fundamental step in sound log interpretation, as it enables the estimation of hydrocarbon saturation (S_h).
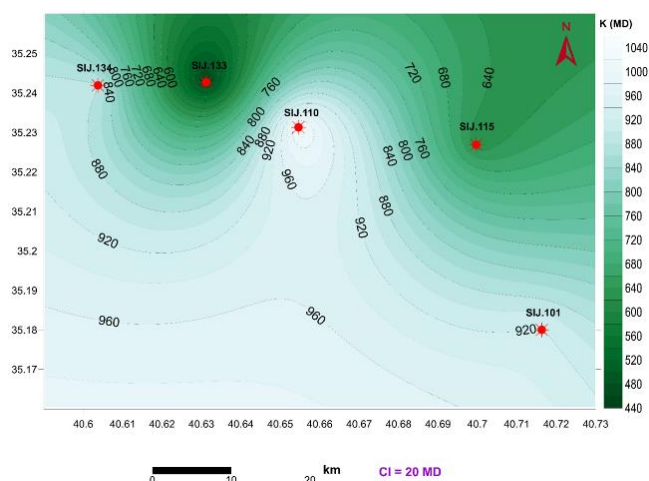
Figure 13. Contour map of the distribution of permeability in the lower Rutbah Formation, Sijan Field

Hydrocarbon saturation (S_h) is a key indicator of the recoverable hydrocarbon volume in a reservoir. To apply Equation (7) for S_w calculation, the formation water resistivity (R_w) must first be determined.

R_w values were obtained using Pickett's plots for each well, where porosity and deep resistivity (R_t) logs were plotted together on log-log scales (Figs. 14a-e).

These plots allowed for the graphical determination of R_w within water-bearing intervals. Due to the large data size, the detailed R_w values for each well are presented in [28].

Water saturation was calculated using these Rw values for all wells, and hydrocarbon saturation was subsequently derived. The results are summarized in Table 5 and displayed as vertical saturation logs in Figures 15a-e. The analysis reveals several intervals with low water saturation, indicating promising hydrocarbon-bearing zones within the Lower Rutbah Formation.

4.5.2. Calculating hydrocarbon saturation

After calculating hydrocarbon saturation (S_h) using Equation (7), the average values of water saturation (S_w) and hydrocarbon saturation for each well were derived and are presented in Table 6. These values were also plotted graphically to visualize their vertical distribution in the Lower Rutbah Formation across the five selected wells (Figs. 15a-e).

Table 5. Average R_w values for each well

Well	SIJ.101	SIJ.104	SIJ.108	SIJ.110	SIJ.115	SIJ.125	SIJ.127	SIJ.129	SIJ.133	SIJ.134
R_w, Ω.m	0.0239	0.0180	0.0149	0.0214	0.00431	0.0296	0.0623	0.0294	0.0277	0.0424

Table 6. Average values of water and hydrocarbon saturations for each well

Well	SIJ.101	SIJ.104	SIJ.108	SIJ.110	SIJ.115	SIJ.125	SIJ.127	SIJ.129	SIJ.133	SIJ.134
S_w	25.6	38.8	35.5	25.8	33.2	26.0	31.8	35.0	39.0	33.0
S_h	74.4	61.2	64.5	74.2	66.8	74.0	68.2	65.0	61.0	67.0

Figure 15 demonstrates the contrast between S_w and S_h along the logged intervals, where zones of low water saturation coincide with high hydrocarbon saturation, especially in wells SIJ.101, SIJ.110, and SIJ.125.

The saturation profiles indicate that hydrocarbon saturation is generally dominant across the studied wells, with S_h values ranging from 61.0 to 74.4%, reflecting good reservoir potential. The highest hydrocarbon saturation values (> 74%) were observed in SIJ.101, SIJ.110, and SIJ.125 are promising zones for hydrocarbon accumulation within the Lower Rutbah Formation.

4.5.3. Horizontal correlation of water and hydrocarbon saturation

Figure 16 represents the distribution of water saturation (S_w) in the Sijan field area, with values between 25 and 39% appearing in a color gradient from dark blue (low saturation) to light blue (high saturation). It can be seen that water saturation is low in the area around well SIJ.101 (26%) and well SIJ.110 (27%), indicating the potential for larger hydrocarbons in these areas, making them promising areas for development. In contrast, high water saturation values (33% and above) appear in areas such as well SIJ.133 and SIJ.134, which may reflect increased water content and reduced reservoir quality. The transparent gradient from low to high water saturation towards the northeast reflects an inhomogeneous distribution of fluids within the reservoir.

Figure 17 represents the distribution of hydrocarbon saturation (S_{hc}) in the Sijan field, with values ranging from 61 to 75%, with a color gradient from light yellow (low values) to dark red (high values).

The map shows high hydrocarbon saturation in the areas surrounding wells SIJ.101 (74%) and SIJ.110 (73%), indicating a high concentration of hydrocarbons, making these areas promising for production. In contrast, values decrease in the areas surrounding wells SIJ.133 (64%) and SIJ.134 (65%), reflecting the lower reservoir quality in these areas. The general trend of hydrocarbon distribution is that values increase towards the southeast, gradually decreasing towards the northwest.

4.5.4. Relationship of porosity and permeability to hydrocarbon saturation in the studied wells

Table 7 shows the reservoir characteristics of five wells in the Sijan field, showing effective porosity (PHIE), permeability (PER), water saturation (S_w), and hydrocarbon saturation (S_h).

Table 7. Comparison of petrophysical properties of the lower Rutbah in the Sijan field, wells (SIJ.101-SIJ.110-SIJ.115-SIJ.133-SIJ.134)

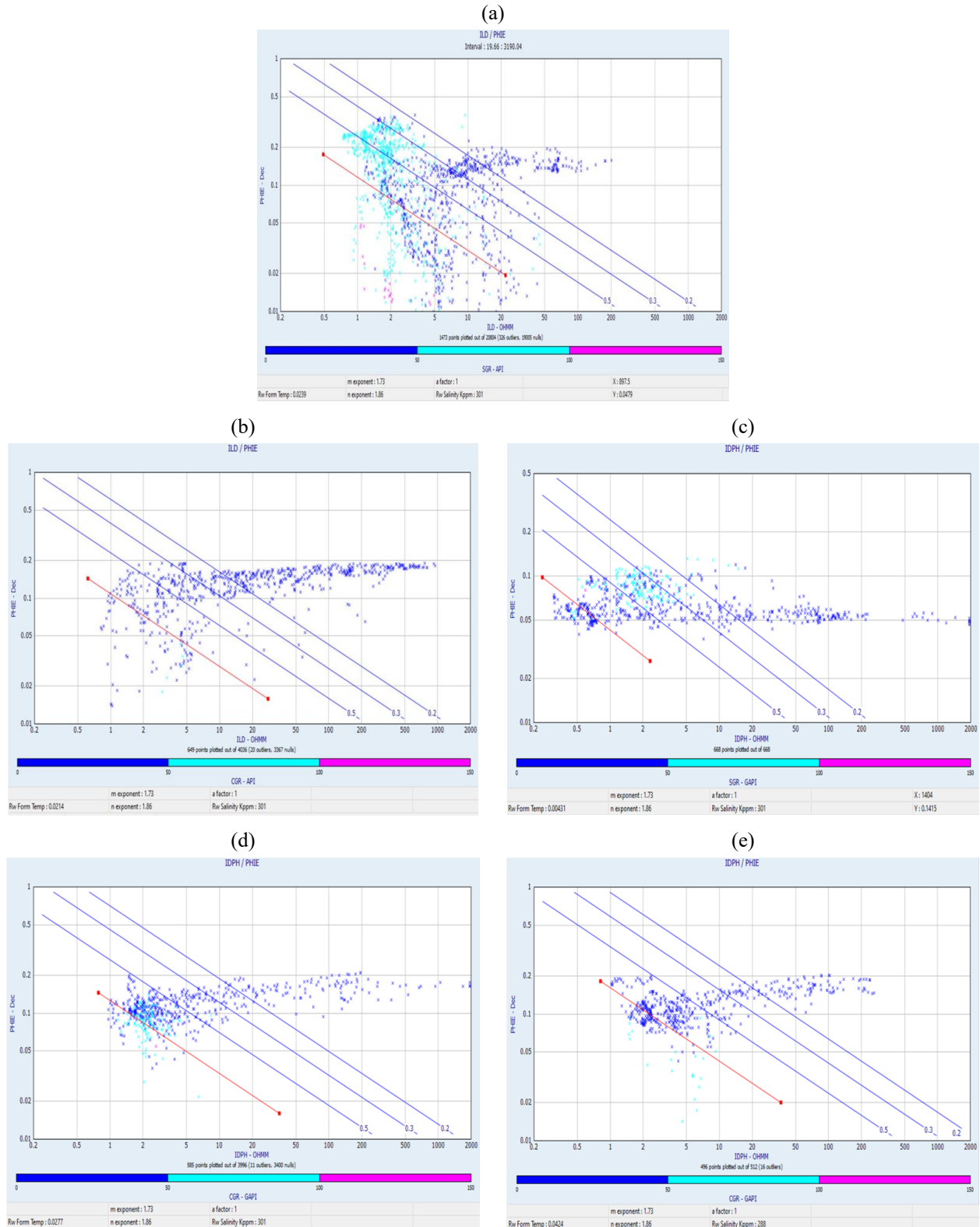| Well name	PHIE, %	K, mD	S_w, %	S_h, %
SIJ.101	10.5	921	25.6	74.4
SIJ.110	12.25	1032	25.8	74.2
SIJ.115	8.5	626	33.2	66.8
SIJ.133	11.0	449	39.0	61.0
SIJ.134	11.3	882	33.0	67.0

(a)

(b)

(c)

(d)

(e)

Figure 14. Determine Rw using Pickett's plots: (a) SIJ.101well; (b) SIJ.110 well; (c) SIJ.115 well; (d) SIJ.133 well; (e) SIJ.134 well

Well SIJ.110 showed the best reservoir characteristics with a high porosity of 12.25% and an excellent permeability of 1032 mD, making it the most efficient for hydrocarbon production. In contrast, well SIJ.115 recorded the lowest porosity of 8.5%, while well SIJ.133 had the lowest permeability of 449 mD, indicating potential fluid transport limitations. In terms of water saturation, well SIJ.101 had the lowest at 25.6%, reflecting the highest hydrocarbon saturation of 74.4%, while well SIJ.133 recorded the highest water saturation of 39% and the lowest hydrocarbon saturation of 61%.

Based on these results, well SIJ.110 can be considered the most suitable for production. At the same time, wells with low permeability and porosity, such as SIJ.133 and SIJ.115, may need reservoir improvements to improve their performance.
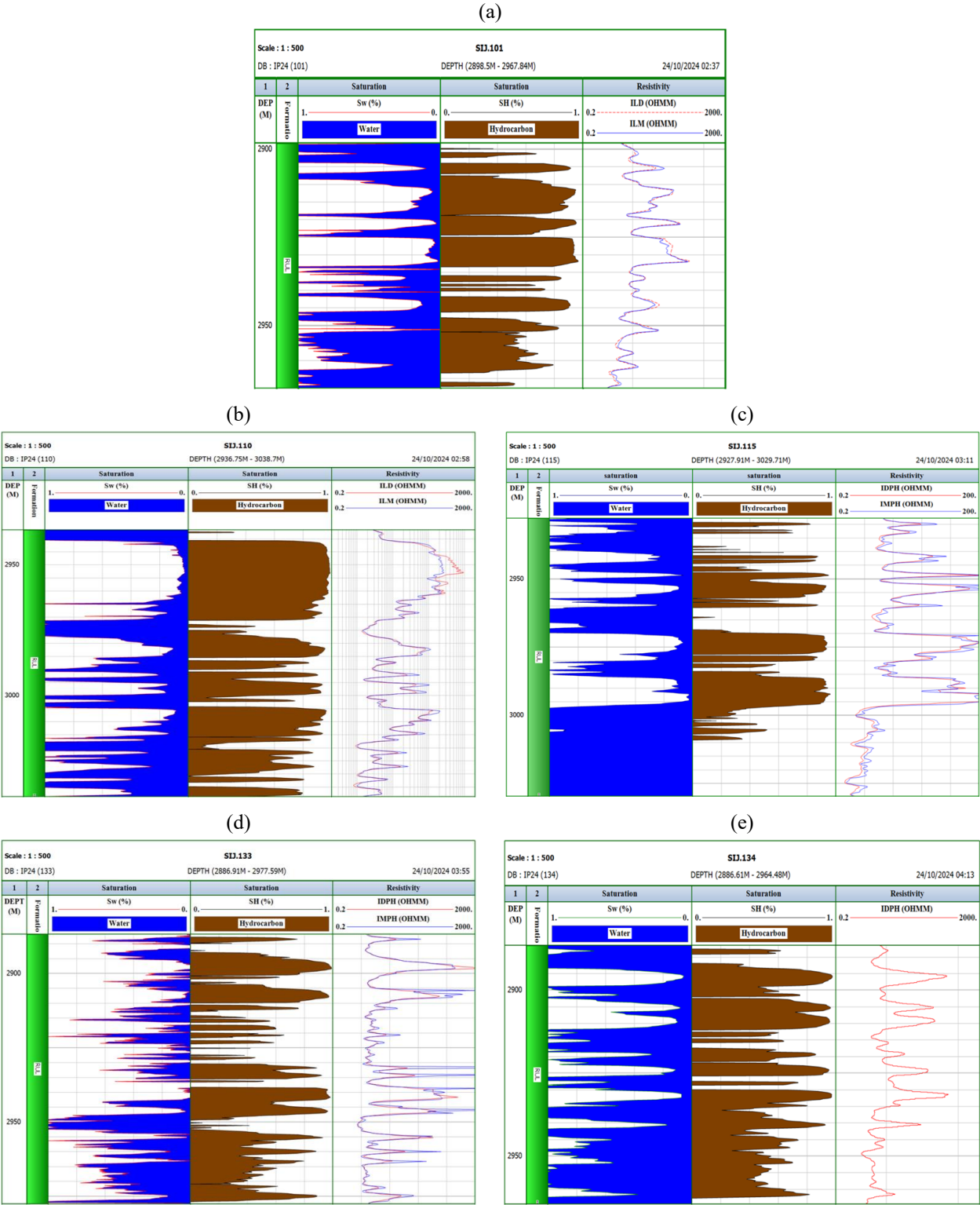
Figure 15. Water and hydrocarbon saturations in lower Rutbah formation: (a) SIJ.101well; (b) SIJ.110 well; (c) SIJ.115 well; (d) SIJ.133 well; (e) SIJ.134 well

5. Conclusions

This study comprehensively analyzed the petrophysical properties of the Lower Rutba Formation in the Sijan Field, Syria, emphasizing their impact on hydrocarbon production potential. The findings have advanced understanding of sandy-clay reservoirs, representing key regional production elements. Using geophysical survey data, porosity, permeability, and the spatial distribution of water saturation and hydrocarbons were thoroughly assessed, providing actionable insights for exploration and production.

The study highlighted the critical role of porosity (PHIE) and permeability (PER) in determining hydrocarbon saturation (S_h). For instance, wells with higher porosity and permeability, such as SIJ.101 (10.5% porosity, 921 mD permeability, and 74.4% hydrocarbon saturation) and SIJ.110 (12.25% porosity, 1032 mD permeability, and 74.2% hydrocarbon saturation), demonstrated superior storage and production potential.
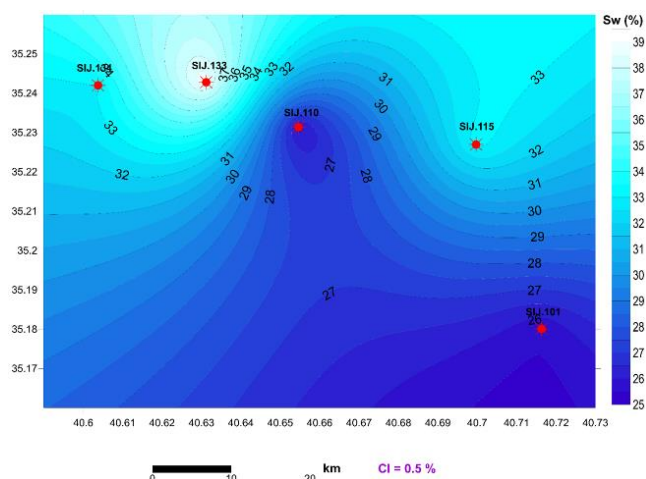
Figure 16. Contour map of the distribution of water saturation in the lower Rutbah Formation, Sijan Field
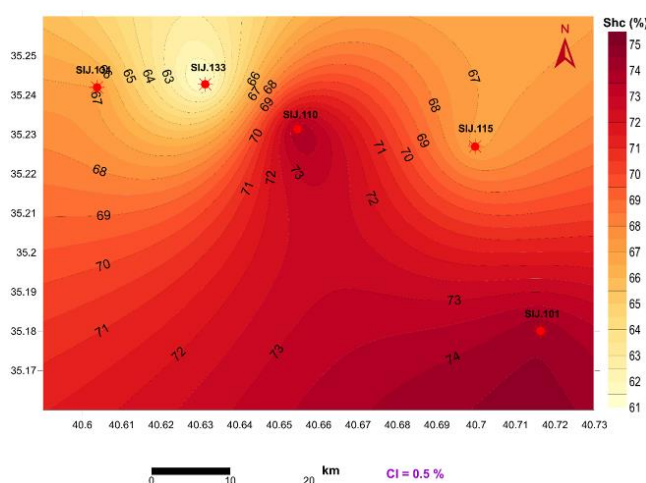

Figure 17. Contour map of the distribution of hydrocarbon saturation in the lower Rutbah Formation, Sijan Field

Conversely, wells with lower permeability, such as SIJ.115 (8.5% porosity, 626 mD permeability, and 66.8% hydrocarbon saturation) and SIJ.133 (11% porosity, 449 mD permeability, and 61% hydrocarbon saturation), exhibited diminished reservoir quality despite moderate porosity. These results underscore the interplay between porosity and permeability in influencing hydrocarbon mobility and reservoir efficiency.

Contour maps revealed zones of high hydrocarbon saturation, offering a foundation for targeted development strategies. Areas around wells SIJ.101 and SIJ.110, with favorable reservoir properties, were identified as ideal candidates for future production. Meanwhile, wells with suboptimal properties, such as SIJ.115 and SIJ.133, may benefit from advanced recovery techniques like hydraulic fracturing to enhance permeability and productivity. Detailed 3D modeling is also recommended to refine spatial understanding of petrophysical properties and guide precise drilling efforts.

This research has provided a practical and cost-effective framework for reservoir evaluation using geophysical logging data. The study bridges the gap between clay distribution and reservoir properties while highlighting the interdependence of porosity, permeability, and hydrocarbon recovery. These insights contribute to optimizing reservoir management by addressing the challenges posed by non-productive rocks.

The development of the Sijan Field hinges on strategies informed by accurate petrophysical data. Areas with favorable properties offer substantial investment opportunities, while regions with average or weak characteristics warrant further exploration and technological intervention. This study's methodology and findings apply to the Sijan Field and offer a scalable global framework for similar fields.

Given the pivotal role of the oil industry in the Syrian economy, adopting the results and recommendations of this study can significantly enhance resource exploitation efficiency. This, in turn, could lead to substantial economic benefits and promote sustainable development in the energy sector, further underscoring the study's importance in advancing regional and global energy strategies.

Author contributions

Funding

Acknowledgements

Conflicts of interest

The authors declare no conflict of interest.

Data availability statement

The original contributions presented in the study are included in the article, further inquiries can be directed to the corresponding author.

References

[1] Caron, C., & Mouty, M. (2007). Key elements to clarify the 110 million year hiatus in the Mesozoic of eastern Syria. *GeoArabia*, *12*(2), 15-36. https://doi.org/10.2113/geoarabia120215

[2] Lai, J., Su, Y., Xiao, L., Zhao, F., Bai, T., Li, Y., & Qin, Z. (2024). Application of geophysical well logs in solving geologic issues: Past, present and future prospect. *Geoscience Frontiers*, *15*(3), 101779. https://doi.org/10.1016/j.gsf.2024.101779

[3] Selley, R.C. (1998). *Elements of petroleum geology*. San Diego, United States: Gulf Professional Publishing, 490 p.

[4] Ibrahem, Y., Morozov, V., El Kadi, M., & Alaa, A. (2023). Porosity enhancement potential through dolomitization of carbonate reservoirs, a case study from the Euphrates Graben fields, East Syria. *Petroleum*, *9*(2), 183-198. https://doi.org/10.1016/j.petlm.2021.05.005

[5] Aldahik, A. (2011). *Crude oil families in the Euphrates graben petroleum system*. Berlin, Germany: Berlin Institute of Technology, 273 p. https://doi.org/10.14279/depositonce-2678

[6] Brew, G., Barazangi, M., Al-Maleh, A.K., & Sawaf, T. (2001). Tectonic and geologic evolution of Syria. *GeoArabia*, *6*(4), 573-616. https://doi.org/10.2113/geoarabia0604573a

[7] Koopman, A. (2005). Regional structural analysis and kinematic framework of the Euphrates graben, East Syria. *International Petroleum Technology Conference*, IPTC-10904-MS. https://doi.org/10.2523/IPTC-10904-MS

[8] Mohannad, R., & AL-Kadi, M. (2018). Petrology and diagenesis study of Rutbah Formation in Omar fields in Euphrates graben. *Al Baath University Journal*, 40, 147-187.

[9] Tickell, F.G., Mechem, O., & McCurdy, R. (1933). Some studies on the porosity and permeability of rocks. *Transactions of the AIME*, 103(01), 250-260. https://doi.org/10.2118/933250-G

[10] Tiab, D., & Donaldson, E.C. (2024). *Petrophysics: Theory and practice of measuring reservoir rock and fluid transport properties*. Oxford, United Kingdom: Gulf Professional Publishing, 950 p.

[11] Schlumberger. (1989). *Log Interpretation Principles / Applications*. Schlumberger Educational Services.

[12] Meslmani, Y. (2010). *Initial national communication of the Syrian Arab Republic*. Damascus, Syrian Arab Republic: United Nations Framework Convention on Climate Change, 164 p.

[13] Barazangi, M., Seber, D., Chaimov, T., Best, J., Litak, R., Al-Saad, D., & Sawaf, T. (1993). Tectonic evolution of the northern Arabian plate in western Syria. *Recent Evolution and Seismicity of the Mediterranean Region*, 117-140.

[14] Litak, R.K., Barazangi, M., Brew, G., Sawaf, T., Al-Imam, A., & Al-Youssef, W. (1998). Structure and evolution of the petroliferous Euphrates graben system, southeast Syria. *AAPG bulletin*, 82(6), 1173-1190. https://doi.org/10.1306/1D9BCA2F-172D-11D7-8645000102C1865D

[15] Barrier, E., Machhour, L., & Blaizot, M. (2014). Petroleum systems of Syria. *Petroleum systems of the Tethyan region: AAPG Memoir*, 106, 335-378. https://doi.org/10.1036/13431862M1063612

[16] Sawaf, T., Al-Saad, D., Gebran, A., Barazangi, M., Best, J.A., & Chaimov, T.A. (1993). Stratigraphy and structure of eastern Syria across the Euphrates depression. *Tectonophysics*, 220(1-4), 267-281. https://doi.org/10.1016/0040-1951(93)90235-C

[17] Brew, G.E., Litak, R.K., Seber, D., Barazangi, M., Sawaf, T., & Al-Imam, A. (1997). Summary of the geological evolution of Syria through geophysical interpretation: Implications for hydrocarbon exploration. *The Leading Edge*, 16(10), 1473-1486. https://doi.org/10.1190/1.1437518

[18] Swiedeh, M.I. (2014). *Facial and sedimentary study of surface and subsurface cretaceous deposits in palmyride chain*. Aleppo, Syria: University of Aleppo.

[19] Alsdorf, D., Barazaugi, M., Litak, R., Seber, D., Sawaf, T., & AI-Saad, D. (1995). The intraplate Euphrates fault system-Palmyrides mountain belt junction and relationship to Arabian plate boundary tectonics. *Annals of Geophysics*, 38(3-4), 385-397. https://doi.org/10.4401/ag-4113

[20] Ibrahem, Y., Morozov, V., El, K.M., & Abdullah, A. (2021). Tectonic and erosion features, and their influence on zonal distribution of the upper Triassic and the lower cretaceous sediments in the Euphrates graben area, Syria. *Geodynamics and Tectonophysics*, 12(3), 608-627. https://doi.org/10.5800/GT-2021-12-3-0541

[21] Alyaseen, M., & Aaney, Y. (2019). Oil and gas potential of the Euphrates Graben in Syria. *Geology. Geophysics. Drilling*, 17(6), 6-14. https://doi.org/10.17122/ngdelo-2019-6-6-14

[22] Austin, O.E., Agbasi, O.E., Samuel, O., & Etuk, S.E. (2018). Cross plot analysis of rock properties from well log data for gas detection in Soku field, Coastal Swamp Depobelt, Niger Delta Basin. *Journal of Geoscience, Engineering, Environment, and Technology*, 3(4), 180-186. https://doi.org/10.24273/jgeet.2018.3.4.1318

[23] Darling, T. (2005). *Well logging and formation evaluation*. Oxford, United Kingdom: Gulf Professional Publishing, 326 p. https://doi.org/10.1016/B978-0-7506-7883-4.X5000-1

[24] Bateman, R.M. (2020). *Formation evaluation with pre-digital well logs*. Elsevier.

[25] Richard, M.B. (2012). *Openhole log analysis and formation evaluation*. Boston, United States: International Human Resources Development Corporation, 661 p.

[26] Ezekwe, N. (2010). *Petroleum reservoir engineering practice*. London, United Kingdom: Pearson Education, 651 p.

[27] Asquith, G.B., Krygowski, D., & Gibson, C.R. (2004). *Basic well log analysis*, American Association of Petroleum Geologists, 16, 31-34. https://doi.org/10.1306/Mth16823

[28] Abudeif, A. (2025). *Global perspectives on evaluating effective porosity and permeability: Insights from hydrocarbon reservoirs in the Lower Rutba Formation, Sejan Field, Syria*. [Data set]. Zenodo. https://doi.org/10.5281/zenodo.15352960

Глобальні підходи до оцінки ефективної пористості та проникності: досвід з нафтових і газових колекторів нижньої частини свити Рутба, родовище Сіян, Сирія

А.М. Абудейф, М.М. Масуд, М.А. Мохаммед, А.Ю. Альхуссейн, М.А. Аббас

Мета. Оцінка петрофізичних характеристик нижньої частини свити Рутба у родовищі Сіян (Сирія) із зосередженням на ефективній пористості та проникності, а також їхньому впливі на продуктивність вуглеводневих покладів для розробки практичної та економічно ефективної моделі оптимізації видобутку вуглеводнів, що сприятиме сталому забезпеченню енергоресурсами і глобальній енергетичній безпеці.

Методика. У дослідженні використано дані геофізичних досліджень каротажу з 10-ти свердловин родовища Сіян. Акустичний, густинний та нейтронний каротаж застосовували для розрахунку пористості й проникності, тоді як водонасиченість визначали за допомогою рівняння Арчі. Проведено порівняльний аналіз між свердловинами для виявлення відмінностей у якості колекторів та визначення зон із високим потенціалом видобутку.

Результати. Отримані дані засвідчили значну неоднорідність петрофізичних властивостей за площею родовища. Визначено, що свердловина SIJ.110 має високу ефективну пористість і проникність, що свідчить про підвищену здатність до накопичення та фільтрації вуглеводнів. Натомість свердловини з підвищеним вмістом глини, такі як SIJ.115, характеризувалися низькою проникністю та зниженими колекторськими властивостями. Побудовано карти насиченості, що ефективно відобразили зони із перспективним потенціалом видобутку вуглеводнів.

Наукова новизна. Запропоновано новий підхід, що інтегрує інтерпретацію каротажних даних і математичне моделювання для оцінки проникності без використання кернових зразків, що дозволяє покращити оцінку колекторів, особливо у піщано-глинистих товщах, і може бути адаптований до подібних геологічних умов у різних регіонах світу.

Практична значимість. Дослідження забезпечує надійну та економічну основу для оцінки якості колекторів, що зменшує залежність від кернових даних, підтримує цілеспрямовану розробку родовищ та сприяє сталому видобутку вуглеводнів завдяки підвищенню ефективності прийняття рішень у системах керування покладами.

Ключові слова: нижня свита Рутба, ефективна пористість, оцінка проникності, вуглеводневі колектори, стале управління ресурсами

Publisher's note